Trans-Golgi network morphology and sorting is regulated by prolyl-oligopeptidase-like protein PREPL and the AP-1 complex subunit μ1A

Karthikeyan Radhakrishnan[1], Jennifer Baltes[1], John W. M. Creemers[2] and Peter Schu[1,*]

[1]Georg-August-University Göttingen, Center for Biochemistry and Moleculare Cell Biology, Biochemie II, Humboldtallee 23, 37073 Göttingen, Germany
[2]K.U. Leuven, Center for Human Genetics, Herestraat 49, 3000 Leuven, Belgium
*Author for correspondence (pschu@gwdg.de)

Accepted 2 January 2013
Journal of Cell Science 126, 1155–1163
© 2013. Published by The Company of Biologists Ltd
doi: 10.1242/jcs.116079

Summary

The AP-1 complex recycles between membranes and the cytoplasm and dissociates from membranes during clathrin-coated-vesicle uncoating, but also independently of vesicular transport. The μ1A N-terminal 70 amino acids are involved in regulating AP-1 recycling. In a yeast two-hybrid library screen we identified the cytoplasmic prolyl-oligopeptidase-like protein PREPL as an interaction partner of this domain. PREPL overexpression leads to reduced AP-1 membrane binding, whereas reduced PREPL expression increases membrane binding and impairs AP-1 recycling. Altered AP-1 membrane binding in PREPL-deficient cells mirrors the membrane binding of the mutant AP-1* complex, which is not able to bind PREPL. Colocalisation of PREPL with residual membrane-bound AP-1 can be demonstrated. Patient cell lines deficient in PREPL have an expanded trans-Golgi network, which could be rescued by PREPL expression. These data demonstrate PREPL as an AP-1 effector that takes part in the regulation of AP-1 membrane binding. PREPL is highly expressed in brain and at lower levels in muscle and kidney. Its deficiency causes hypotonia and growth hormone hyposecretion, supporting essential PREPL functions in AP-1-dependent secretory pathways.

Key words: Adaptin, Clathrin, Prolyl-oligopeptidase, Sorting, Trans-Golgi network

Introduction

AP-1 mediates clathrin-coated transport vesicle (CCV) formation and protein sorting, between the trans-Golgi network (TGN) and endosomes. AP-1 and the plasma membrane AP-2 recycle between membranes and the cytoplasm during transport vesicle formation and vesicle uncoating, together with clathrin. Importantly, they also recycle independent of vesicle formation and clathrin, indicating abortive CCV formation events, which have been described in detail for the homologous AP-2 at the plasma membrane (Loerke et al., 2009; Wu et al., 2003). CCV uncoating is mediated by Hsc70 and its co-chaperones auxilin 1 (DNAJC6) and auxilin 2 (cyclin-G-associated kinase, GAK) (Hirst et al., 2008). Hsc70 binds to a short peptide-motif in the clathrin-heavy-chain inducing clathrin basket disassembly (Rapoport et al., 2008). Less is known about mechanisms regulating the subsequent membrane dissociation of the AP complexes.

High-affinity AP-1 membrane binding requires three components, and loss of just one of them, leads to the loss of AP-1 membrane binding *in vivo*. These are a cargo protein with an AP-1-binding motif, phosphatidylinositol 4-phosphate (PI-4-P) and the small GTP-binding protein Arf-1^{GTP} (Heldwein et al., 2004; Robinson and Kreis, 1992; Rohde et al., 2002; Wang et al., 2003). All four AP-1 adaptin subunits are involved in binding of those factors. μ1A and σ1 adaptins bind cargo proteins, whereas the putative PI-4-P binding domain has been identified in γ1. The N-terminal core domains of γ1 and β1 adaptins bind to Arf-1^{GTP} (Austin et al., 2002; Meyer et al., 2005; Shinotsuka et al., 2002). Clathrin cage formation is mediated by clathrin recruitment via binding to the β1 'hinge-ear' domain and the γ1 N-terminal core domain (Doray and Kornfeld, 2001; Gallusser and Kirchhausen, 1993). Clathrin stabilises the coat and clathrin cage assembly contributes energy for the membrane deformation and vesicle budding (Dannhauser and Ungewickell, 2012).

In addition to cargo binding, μ1A adaptin is involved in the regulation of membrane–cytoplasm recycling of AP-1 (Medigeshi et al., 2008). Homologies between μ1A of AP-1 and μ2 of AP-2 range from 25% to 50%, indicating that subdomains fulfil AP-complex specific functions. Therefore we constructed chimeras, in which domains in μ1A were replaced by the corresponding μ2 domains and expressed these in μ1A−/− fibroblasts. Only the chimera with a domain swap of the N-terminal seventy amino acids, which have with 25% the lowest sequence homology, was stably incorporated into an AP-1 complex, named AP-1*. Analysis of AP-1* membrane-cytoplasm recycling revealed that the N-terminus of μ1A is involved in the regulation of AP-1 membrane-cytoplasm recycling. The recycling rate is reduced and this lowers the sorting fidelity of mannose-6-phosphate receptors and a fraction of cathepsin D is secreted (Medigeshi et al., 2008). The μ1A N-terminus is not oriented towards the membrane, but to the cytoplasm and can not influence membrane binding directly and has to bind to additional proteins.

AP-complexes have been shown to exist in two conformations. The 'open' conformation has the cargo binding domains exposed and in the 'closed' conformation shielded. The transition between

Journal of Cell Science

Journal of Cell Science

the two forms is supported by μ-adaptin phosphorylation (Owen and Evans, 1998; Owen et al., 2001). This enables γ1 and β1 to undergo a rotation releasing the cargo-binding motif in the σ-adaptins. This rotation moves the cytoplasm oriented domains of both large adaptins closer together (Collins et al., 2002; Conner and Schmid, 2002; Ghosh and Kornfeld, 2003; Höning et al., 2005; Jackson et al., 2010; Motley et al., 2006; Ricotta et al., 2002). The μ1A adaptin N-terminus is positioned at the bottom of this celft and is therefore only readily accessible in the 'closed' conformation of the complex. The membrane bound pool of AP-1* is in the closed conformation and can not bind to cargo proteins via the motifs in μ1A and σ1 (Medigeshi et al., 2008). This indicates low-affinity AP-1* membrane binding mediated only by $Arf1^{GTP}$ and PI-4-P, but in spite of this membrane recycling rates are reduced.

Arf1-GTPase is activated by Arf1-GAP, which itself can be activated by the high membrane curvature generated during vesicle formation (Ambroggio et al., 2009). Thus without transport vesicle formation $Arf\text{-}1^{GTP}$ will not be inactivated and will tether AP-1 on the membrane. The PI-4-P binding motif in γ1 is not well characterised and it is not clear whether induction of conformational changes regulates binding affinities. In addition to the these two modes of membrane binding, AP-1 binds to many proteins via the C-terminal 'ear' domains of γ1 and β1, the network of 'accessory'-proteins, which undergoes phosphorylation–dephosphorylation during the process of membrane–cytoplasm recycling (Ghosh and Kornfeld, 2003; Ricotta et al., 2008; Ungewickell and Hinrichsen, 2007). Accessory proteins can be co-adaptors, binding cargo not recognised by AP complexes, but they also contribute to vesicle formation. The small 'ear' domains cannot and do not bind all these proteins at the same time and they are thus recruited subsequently (Loerke et al., 2011; Taylor et al., 2011). Despite this orchestration of the events, many CCV formations do not proceed until the end and are aborted (Liu et al., 2009; Loerke et al., 2009). How these most likely imperfect coats are removed or disassembled is not known. The data on AP-1* membrane binding and recycling indicate that the μ1A N-terminus can play a role in this process. None of the proteins known so far to influence AP-1 membrane binding interacted with this domain (Medigeshi et al., 2008).

The N-terminal seventy amino acids of μ1A are located at the bottom of the cleft formed by γ1 and β1, and are accessible only from the cytoplasmic face of the complex. In the open, cargo bound, conformation this cleft is narrower, limiting access to the μ1A N-terminus. We reasoned that the μ1A N-terminus binds a cytoplasmic protein and that this interaction induces conformational changes in the AP-1 complex weakening its membrane binding and supporting its membrane dissociation.

We searched for proteins interacting with this domain by using the N-terminal seventy amino acids of μ1A as bait in a yeast two-hybrid library screen. We isolated a putative prolyl-oligopeptidase, which had been named PREPL for prolyl-oligopeptidase-like protein. PREPL is a soluble cytoplasmic protein of unknown function, with highest expression in brain, intermediate expression in muscle and kidney and very low expression elsewhere. Its deficiency is associated with the Hypotonia-Cystinuria syndrome (HCS), characterised by hypotonia and growth hormone hyposecretion, causing retardation of infantile development. Although its sequence homology predicts a hydrolytic activity and despite the binding of peptidase inhibitors, peptides cleaved by the protein could not be identified yet (Martens et al., 2006). We demonstrate a PREPL effector function on the redistribution of AP-1 from membranes into the cytoplasm. This points to tissue-specific PREPL–AP-1-dependent pathways underlying the hypotonia and GH-hyposecretion syndromes of HCS.

Results

$\mu1A\text{-}N^{1\text{-}70}$ binding protein

We used the μ1A adaptin N-terminal 70-amino-acid-long domain ($\mu1A\text{-}N^{1\text{-}70}$) (Fig. 1A–C) as a bait in a yeast two-hybrid library

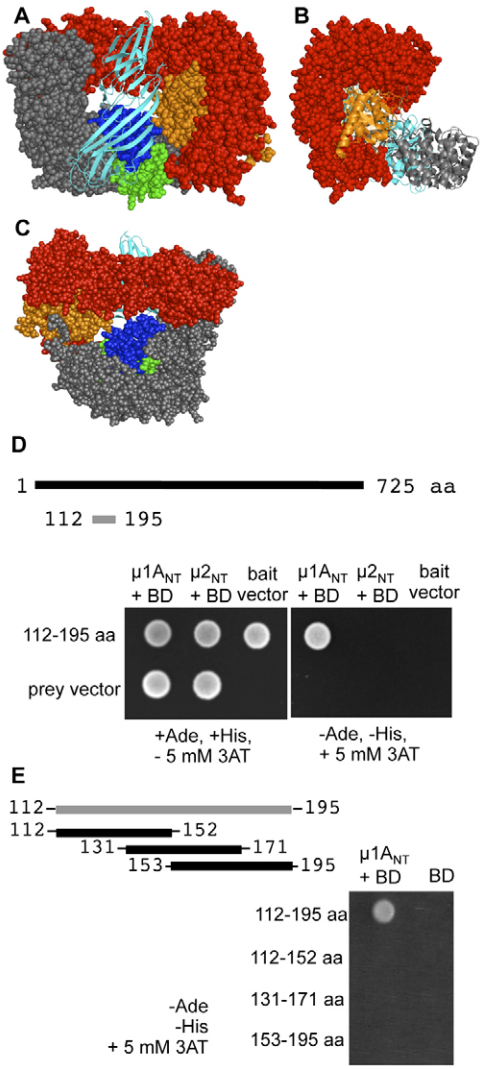

Fig. 1. Clone isolated in a Y2H library screen with the N-terminus of μ1A as bait. (**A**) Position of the N-terminal 70 aa of μ1A in the AP-1 complex (Heldwein et al., 2004). μ1A domains: $\mu1A\text{-}N^{1\text{-}70}$ PREPL binding domain, blue; $\mu1A\text{-}N^{71\text{-}150}$ domain, green; C-terminal cargo-binding domain, cyan; γ1, red; β1, grey; and σ1, gold. Membrane would be below the complex. (**B**) Side view of the AP-1 cleft formed by the two large adaptins of a cargo-free complex. The μ1A N-terminus is exposed at the bottom of the cleft (software Pymol). (**C**) Cytoplasmic face of the complex. (**D**) Binding of 83 aa fragment of the 725 aa protein binding μ1A, but not μ2. Cell growth is not blocked by addition of the His3p competitive inhibitor (3AT); (**E**) Binding to μ1A requires the entire 83 aa (112–195) of the 725 aa protein PREPL. BD, binding domain.

Journal of Cell Science

screen with a mouse embryonic cDNA library as prey. A total of ~10^6 clones were screened (Behrens et al., 1998). 44 were positive for all four reporter genes of the yeast tester-strain AH109, out of which 16 clones were unique, but one clone was identified 18 times. This clone could be verified by retesting and binding was stable in the presence of 5 mM 3-AT (Fig. 1D). The insert encoded 83 amino acids of the N-terminal domain of PREPL (Fig. 1D). It did not bind to the N-terminal 70 amino acids of μ2 (Fig. 1D). Splitting of this domain into three fragments (aa 112–152, aa 131–171 and aa 153–195) resulted in the loss of μ1A binding (Fig. 1E). This indicates that residues mediating μ1A binding do not form a short sequence motif, but are distributed within this larger domain.

Next we tested for direct AP-1 binding to PREPL *in vivo* by co-immunoprecipitation experiments. First, we tested for PREPL and AP-1 crosslinking efficiencies. AP-1 and AP-1* expressing MEF cell lines were incubated with the membrane permeable crosslinker DSP for 30 minutes on ice and cell lysates were analysed by western blots developed with anti-PREPL and anti-γ1 antisera (AP-1) after they were separated under reducing and non-reducing conditions. In both cell lines all PREPL proteins migrated in a ~300 kDa protein complex and under reducing conditions, they all migrated as the native long and short forms of the protein, demonstrating highly efficient crosslinking of PREPL. Nearly all γ1 adaptins migrated to the very same position (supplementary material Fig. S1A). The calculated mass of the heterotetrameric AP-1 complex is 268 kDa and therefore proteins have been crosslinked to AP-1 and possibly also PREPL. We performed anti-PREPL immunoprecipitations after [^{35}S]methionine metabolic labelling and crosslinking. This revealed binding of a number of different proteins from ~10 kDa to 110 kDa to PREPL (supplementary material Fig. S1B). This demonstrated highly efficient PREPL crosslinking to a number of proteins, but this complex protein pattern makes it difficult to interpret a co-IP as a direct interaction of PREPL with AP-1. In addition, membrane bound AP-1 is part of a complex proteinaceous coat and has many different binding partners, which themselves have a complex interactome.

We also prepared protein extracts from mouse brain for the anti-PREPL co-immunoprecipitations experiments, because it is the tissue of highest PREPL and AP-1 expression (Glyvuk et al., 2010; Martens et al., 2006). We used cytosolic as well as membrane fractions for the co-immunoprecipitation experiments, because the AP-1* data predict preferential PREPL binding to a membrane bound AP-1 pool, which is also indicated by the altered AP-1 membrane localisation upon PREPL overexpression or PREPL deficiency shown below. Besides MEF and brain cytosol, we used brain membrane fractions from 10,000 ***g*** and 14,000 ***g*** supernatants for the experiments and immuncomplexes were isolated using protein G-coated magnetic beads to avoid centrifugation steps. γ1 (AP-1) was not detected in the isolates from the brain 14,000 ***g*** supernatant or from the crosslinked MEF cytosolic fractions (data not shown). This indicates that PREPL and AP-1 do not interact in the cytoplasm or that such an interaction is only very transient. However, AP-1 was enriched in the isolate from the 10,000 ***g*** brain supernatant. 12% of total AP-1 complexes were found in the PREPL IP fraction (Fig. 2). We also analysed cortex and brainstem separately, because the delayed development of PREPL-deficient patients suggests essential functions in the brainstem, but results were identical for both (data not shown). Also AP-2 (anti-α adaptin) was

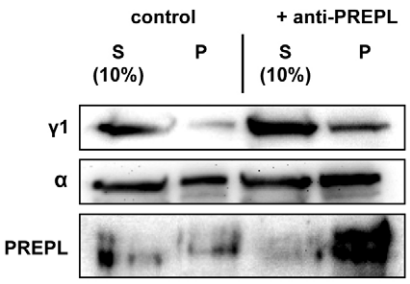

Fig. 2. AP-1 (γ1) is immuno-isolated from mouse brain 10,000 *g* supernatant fraction with anti-PREPL antisera. 10% of the supernatant fraction was loaded as input control. See Results section for details. S, supernatant; P, pellet.

enriched in this fraction. This indicates PREPL binding also to a protein binding AP-1 as well as AP-2. Membrane bound AP-1 is part of a complex protein coat and has an extensive interactome. The composition of the AP-1 coat even changes during transport vesicle formation. Thus a spatial proximity and crosslinking of PREPL and AP-1 could be mediated by binding of both to a third protein or to even two different proteins binding each other. Therefore it is impossible to demonstrate an individual direct protein–protein interaction of these proteins *in vivo*. Cytoplasmic PREPL and cytoplasmic AP-1 seem not to form complexes stable enough to be demonstrated by co-IP or crosslinking. In fact, there are several examples in the literature, which demonstrate that one protein has to be in contact with a membrane for complex formation, even so membrane binding does not induce extended conformational changes (Lo et al., 2012). Importantly, however, the isolation of membrane bound proteins by anti-PREPL serum demonstrates that the soluble, cytoplasmic PREPL interacts with membranes coated with AP-1.

PREPL induced redistribution of AP-1

To test for *in vivo* AP-1/PREPL interaction we first tested for effects of PREPL overexpression on AP-1 membrane–cytoplasm distribution and for their co-localisation. PREPL expression is highest in brain and it is expressed to a lesser extent in kidney, heart and skeletal muscle, whereas only trace amounts are found elsewhere (Jaeken et al., 2006). We used mouse embryonic fibroblast (MEF) cell lines with comparable low endogenous PREPL expression for the experiments, because it enabled us to use AP-1* expressing cells as controls. AP-1* should not be sensitive to PREPL overexpression according to the Y2H data (Fig. 1D). We expressed full-length murine PREPL with a C-terminal HA tag transiently in MEF cells, which localised to the cytoplasm as previously reported. The overexpression resulted in severely reduced peri-nuclear TGN binding of AP-1 (Fig. 3). AP-1 membrane binding was lost completely in 10% of the transfectants and 90% showed severely reduced membrane localisation due to variable PREPL expression levels. We quantified the residual AP-1 membrane binding by normalising the signal intensity for the TGN area and by determining maximal signal intensity, marking domains with high AP-1 membrane density, as well as the minimal signal intensity, marking membrane domains with comparable few AP-1 complexes bound. This revealed a reduction of intensity/area and the maximal intensity signal to 55% of wild type on average, whereas the minimal signal intensity was reduced down to 25%

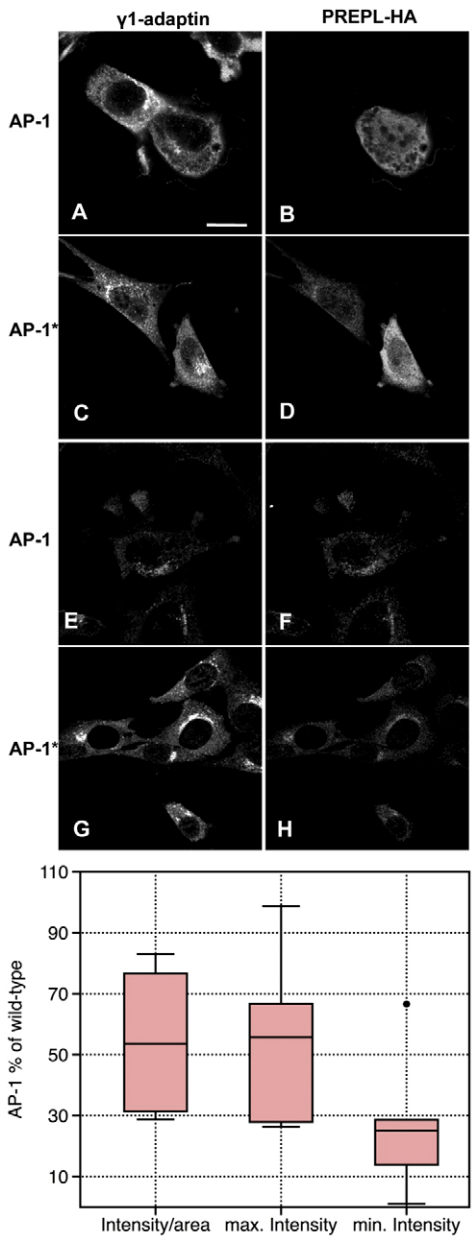

Fig. 3. PREPL-HA overexpression in AP-1 and in AP-1* cell lines. (**A–D**) Transient PREPL expression. (**E–H**) Stable PREPL expression. Left panels: γ1 (AP-1) staining. Right panels: PREPL-HA staining. Scale bar: 20 μm. Box-blot diagram shows residual AP-1 membrane binding in MEF cells with transient PREPL overexpression, expressed in % of wild-type AP-1 (γ1) IF signal intensities. Shown are the reduction in the AP-1 signal intensities normalised for the TGN area and the maximal and minimal signal intensities of AP-1 at the TGN ($n=7$).

on average ($n=7$; Fig. 3). This indicates that membrane domains covered with comparably fewer AP-1 complexes are more sensitive to PREPL induced redistribution into the cytoplasm. As expected membrane binding of AP-1* was not reduced, in line with the PREPL binding specificity determined in the Y2H assay (Fig. 3). This indicates that the slower membrane– cytoplasm recycling rate of AP-1* is due to impaired binding of PREPL to AP-1* (Medigeshi et al., 2008). PREPL appears to induce AP-1 membrane dissociation. We did not observe peripheral membranes labelled with AP-1, which would indicate a PREPL/AP-1 induced TGN fragmentation. PREPL/AP-1 binding could also lead to the destruction of the entire TGN. However, this would destroy the essential biosynthetic pathway and would inevitably lead to cell death. We observed rapid declining expression levels of PREPL in the transfectants, but did not detect any signs of cell death, which makes this alternative explanation highly unlikely. Next, we established cell lines with stable and thus low PREPL-HA expression and also under these conditions a reduction of AP-1 membrane binding is observed, whereas AP-1* membrane binding was unchanged, confirming the effect of PREPL overexpression on AP-1 membrane binding (Fig. 3). Under these low PREPL expression levels, co-localisation of PREPL with residual membrane bound AP-1 (Fig. 3), as well as with AP-1* (Fig. 3), was detectable. PREPL colocalisation with AP-1* indicates that it is able to bind weakly to additional AP-1 domains, or to a third protein binding also AP-1. Importantly, PREPL is not detected on the TGN in the absence of AP-1 and therefore PREPL binding to the TGN, as well as its binding to a putative third protein, is AP-1 dependent. These *in vivo* data do confirm a function of a direct binding of PREPL to AP-1 as indicated by the direct and specific PREPL-μ1A binding in the Y2H analysis.

PREPL 'knockdown' and AP-1 membrane binding

If PREPL is involved in the regulation of AP-1 membrane–cytoplasm recycling and induces AP-1 redistribution into the cytoplasm, PREPL-deficiency should lead to an increased pool of membrane bound AP-1. To test this, we established RNAi mediated PREPL 'knockdown' in HeLa cells, using four sequences predicted to mediate a 'knockdown' of human PREPL. These were tested for downregulation by western blot 24 and 48 hours post-transfection. Only oligonucleotide 4 (Prepl 4) led to a reproducible reduction in protein levels down to 20–30% of wild type (Fig. 4A). Prolonged incubation times did not lead to further downregulation. Prepl-oligonucleotides 1, 2 and 3 led to downregulation of PREPL expression to 50–60% of wild type. In the experiments, Prepl1, standard lamin oligonucleotide and mock-transfected cells all served as negative controls. AP-1 membrane binding (anti-γ1) was analysed by indirect immunofluorescence microscopy 24 hours post-RNAi transfection. We observed more intense AP-1 membrane staining in the PREPL 'knockdown' cells at steady state (Fig. 4B,C). Quantification of signal intensities revealed an average 1.7 ± 0.23-fold ($n=10$) increase in membrane bound AP-1 in Prepl 4 transfected cells compared to mock-transfected control cells (1.0 ± 0.26; $n=7$). In Prepl1-transfected control cells (50–60% PREPL 'knockdown'), AP-1 membrane binding was 1.1 ± 0.3 ($n=14$) compared to the mock-transfected control cells (Fig. 4C). This 1.7-fold increase in the AP-1 membrane bound pool is comparable to the 1.5-fold increase in AP-1 membrane binding determined in an auxilin1/auxilin2 double 'knockdown' in HeLa cells, in which Hsc70 induced clathrin uncoating is blocked (Hirst et al., 2008). The severe protein sorting defects in these cells are however due to the depletion of the cytoplasmic pool of free clathrin by clathrin basket formation in the cytoplasm. The effect of PREPL 'knockdown' on AP-1 membrane-cytoplasm recycling was not as severe as the altered recycling rate of the mutated AP-1 complex AP-1*. We could not reliably determine a delay in brefeldin A induced AP-1 redistribution into the cytoplasm, as it had been determined for

Journal of Cell Science

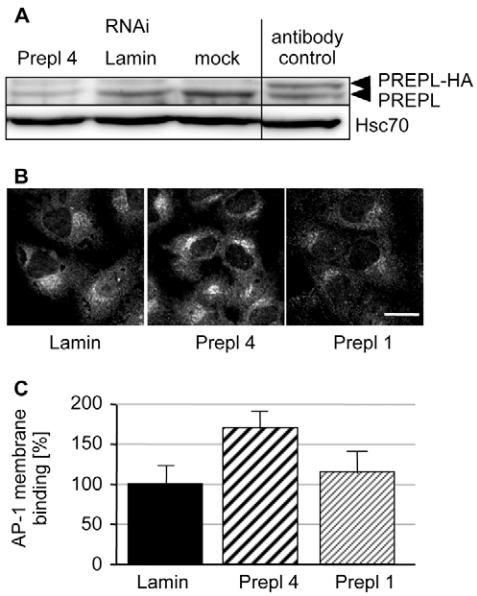

Fig. 4. RNAi-mediated PREPL 'knockdown' in HeLa cells and AP-1 membrane binding. (**A**) PREPL 'knockdown' analysed by western blot. Expression of the murine PREPL-HA-tagged protein demonstrates anti-serum specificity (last lane: huPREPL, murine PREPL-HA). Hsc70 staining served as control. (**B**) Indirect immunofluorescence microscopy for AP-1 membrane binding (γ1) in lamin, Prepl 4 and Prepl 1 (insufficient PREPL 'knockdown') transfected cells. Scale bar: 20 µm. (**C**) Quantification of AP-1 membrane binding in lamin (±26%; $n=7$), Prepl 4 (±23%; $n=10$) and Prepl 1 (±30%; $n=14$) transfected cells.

AP-1* (Medigeshi et al., 2008). This is most likely due to the variable amounts of residual PREPL present in these cells. Human patient cell lines lacking PREPL did show altered AP-1 recycling (see below). Thus, reducing PREPL expression leads to redistribution of AP-1 onto membranes as predicted by the reduced AP-1 membrane binding upon PREPL overexpression and by the increased membrane binding of AP-1*, which is not able to bind PREPL.

PREPL subdomain functions

A short sequence of the PREPL N-terminus binds µ1A. To test whether this domain is sufficient for AP-1 redistribution or whether additional PREPL domains are required, we expressed HA-tagged PREPL subdomains. These were chosen based on sequence homologies to the porcine prolyl-oligopeptidase PREP, because the crystal structure of this family member has been solved (Fig. 5; supplementary material Fig. S2) (Szeltner et al., 2002). The structure reveals three subdomains: an N-terminal helix formed by amino acids 1–88, an N-terminal β-propeller domain and a C-terminal peptidase S9 α/β fold domain. The N-terminal helix is layered on top of the peptidase S9 α/β fold domain and continues to the N-terminal β-propeller domain, thereby connecting the two subdomains (Fig. 5, green). This domain is absent in the short form sPREPL, which starts with Met^{89} of PREPL (Jaeken et al., 2006; Parvari et al., 2005). The PREP catalytic triad is located at the bottom of the peptidase S9 α/β fold domain facing the top of the N-terminal β-propeller domain (Fig. 5, red sticks). Therefore, the protein has to undergo conformational changes to make the catalytic centre accessible. Either the propeller domain opens up to create a channel for the

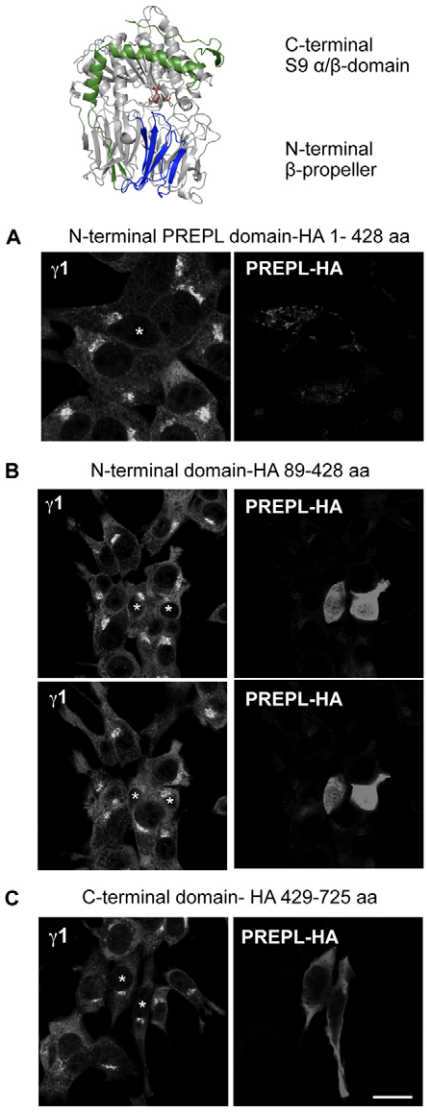

Fig. 5. Expression of PREPL subdomains in AP-1-expressing cells. Subdomains were cloned based on the PREP crystal structure. PREP structure is coloured: N-terminal extension of the β-propeller in green, the corresponding µ1A-binding domain of PREPL in blue, catalytic triad in the C-terminal domain as red sticks. (**A**) Full-length N-terminal β-propeller domain-HA (1-428 aa). (**B**) N-terminal β-propeller domain-HA truncated by the N-terminal helix formed by amino acids 1–88. Two confocal sections of the same cells are shown. (**C**) C-terminal peptidase S9 family α/β fold domain-HA formed by amino acids 429–725. Scale bar: 20 µm.

peptide, or the two domains fold up to expose the catalytic centre, as it has been demonstrated for a bacterial family member (supplementary material Fig. S2) (Shan et al., 2005). Thus PREPL could be a mechanoenzyme and these structural changes could be involved in the molecular mechanism supporting AP-1 redistribution. The PREPL domain binding the µ1A-$N^{1–70}$ corresponds to β-sheets of the β-propeller domain of PREP (Fig. 5, blue). We expressed the predicted PREPL N-terminal β-propeller domain, with and without the N-terminal helix domain, and the C-terminal peptidase S9 α/β like domain with C-terminal HA tags (Fig. 5). Neither N-terminal domain caused a redistribution of AP-1, nor did they show colocalisation with

Journal of Cell Science

AP-1 on membranes in any of the transfectants (Fig. 5A,B). While the propeller domain alone was distributed throughout the cytoplasm, the propeller with the N-terminal extension was not. It appears to bind to peripheral organelles, where the N-terminal extension may bind to a protein homologous to the C-terminal domain of PREPL. Therefore, a contribution of the first 88 amino acids to the induction of AP-1 redistribution cannot be excluded, however they do not contribute to PREPL targeting to AP-1. The C-terminal peptidase S9 α/β like domain was cytoplasmic too and did not induce AP-1 redistribution into the cytoplasm in any of the transfectants (Fig. 5C). Thus, full-length PREPL is required for *in vivo* AP-1 binding and its redistribution into the cytoplasm. This indicates that additional AP-1 interaction domains besides the μ1A N-terminus exist or that PREPL binds to a third protein, forming a trimeric X-PREPL–AP-1 complex. This is in line with the low, residual colocalisation of PREPL with AP-1* (Fig. 3).

PREPL catalytic triad function

Human PREPL was tested for prolyl-oligopeptidase activity, but no substrate was identified yet, despite the specific binding of peptidase inhibitors (Jaeken et al., 2006; Szeltner et al., 2005). The Ser-Asp-His catalytic triad appeared to be conserved in PREPL (supplementary material Fig. S2). Modelling the PREPL structure on the porcine PREP structure as template resulted in a structure resembling only part of the peptidase S9 α/β catalytic domain, which does not include the entire putative Ser-His-Asp catalytic triad, indicating that PREPL may not be catalytically active.

Nevertheless, we tested for a function of the putative enzymatic activity in AP-1 redistribution and replaced the conserved nucleophilic Ser557 by Ala. Transient overexpression of PREPL-HA Ser557Ala revealed Ser557-independent AP-1 redistribution from the membrane to the cytoplasmic pool (Fig. 6; supplementary material Fig. S3). Residual AP-1 membrane binding of ~60% was detectable in most clones (88%, $n=7$) as it was for wild-type PREPL expression. Also AP-1* was not affected (supplementary material Fig. S3). Thus a contribution of a putative hydrolytic activity cannot be excluded, but it is not essential. Therefore the major conformational changes

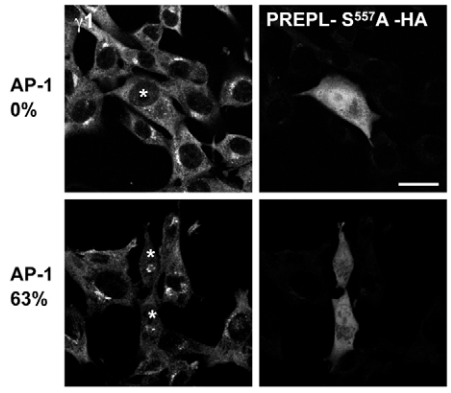

Fig. 6. AP-1 redistribution by expression of the PREPL-Ser557Ala putative catalytic domain mutant in MEF cells. Left: AP-1 (γ1) staining. Right: anti-PREPL-Ser557Ala-HA staining. Depending on PREPL expression levels, AP-1 is removed from membranes either completely or by ~40% (see additional AP-1 and AP-1* cells in supplementary material Fig. S3). Asterisks mark PREPL-expressing cell. Scale bar: 20 μm.

this protein family is able to undergo should be involved in the redistribution of AP-1 into the cytoplasm.

Interestingly, also the N-terminal domain of PREP has a function independent of its peptidase activity. PREP 'knockout' mice show altered neuronal growth cone morphology, which can be rescued by peptidase-deficient PREP. PREP inhibitors improve learning and memory and it has always been assumed that this is due to altered neuropeptide processing, however PREP is cytosolic. Inhibitor binding to the catalytically active site may induce scissor closing (supplementary material Fig. S2). This change can alter PREP interactions with cytoplasmic target proteins and can explain the physiological effects of the inhibitors (Di Daniel et al., 2009).

PREPL deficiency

The *PREPL* gene is one of two neighbouring loci affected by a microdeletion in patients with hypotonia-cystinuria syndrome (HCS; MIM 606407). The second gene is *SLC3A1* (solute carrier family 3, member 1), which encodes the large subunit of an amino acid transporter for cystine and dibasic amino acids (Jaeken et al., 2006; Martens et al., 2006). We used primary human fibroblasts from two HCS patients (HCS 14 and 16), which do not express PREPL and from two healthy controls (ct 8 and 10) to analyse the effect of PREPL deficiency on AP-1 membrane–cytoplasm distribution (supplementary material Fig. S4A) (Jaeken et al., 2006). AP-1 staining revealed intense labelling of a dramatically spread out trans-Golgi network in patient fibroblasts (Fig. 7A). We quantified this and determined the size of the TGN relative to the size of the nucleus. This revealed a 2.5-fold increase in the TGN area (Fig. 7B; wt $n=10$, ΔPREPL $n=9$). This phenotype was fully rescued by expression of the murine, HA-tagged PREPL (Fig. 7B, $n=9$ and Fig. 7D). Ectopic PREPL expression in these deficient cells reduces the area of the AP-1 labelled TGN below that of the controls and also reduces the variability in size. We observed also in the HeLa cell 'knockdown' experiments a more spread out TGN, but it was not as pronounced and heterogeneous, presumably due to residual PREPL, and thus we did not quantitate this observation (J.B.). Brefeldin A induced AP-1 redistribution into the cytoplasm revealed a readily visible incomplete AP-1 redistribution in both PREPL-deficient cell lines compared to the two controls (Fig. 7C; supplementary material Fig. S4B), as it has been observed for AP-1* in mouse embryonic fibroblasts (Medigeshi et al., 2008). Quantification of the reduction in the AP-1 signal intensities in these four human cell lines revealed a reduction of AP-1 membrane binding below 20% in the control cell lines after 5 and 10 minutes in the presence of BFA, whereas PREPL-deficient cell lines retained ~60% of their AP-1 on the TGN after 5 and 10 minutes (Fig. 7C). This factor of ~3 correlates with the ~2.5-fold increase in TGN area and it demonstrates PREPL-dependent as well as PREPL-independent AP-1 membrane dissociation.

We analysed cathepsin D sorting by pulse-chase experiments, because AP-1* expressing cells missort the Golgi precursor form of cathepsin D into the culture medium (Medigeshi et al., 2008). Surprisingly, pro-cathepsin D is not secreted by the PREPL-deficient cell lines. However, pro-cathepsin D processing appears to be slightly delayed in these cells, indicating slower TGN-endosome-lysosome sorting (supplementary material Fig. S4C). This can be explained by an adaptation of the patient fibroblasts to the PREPL deficiency. Adaptations induced by complete loss

Journal of Cell Science

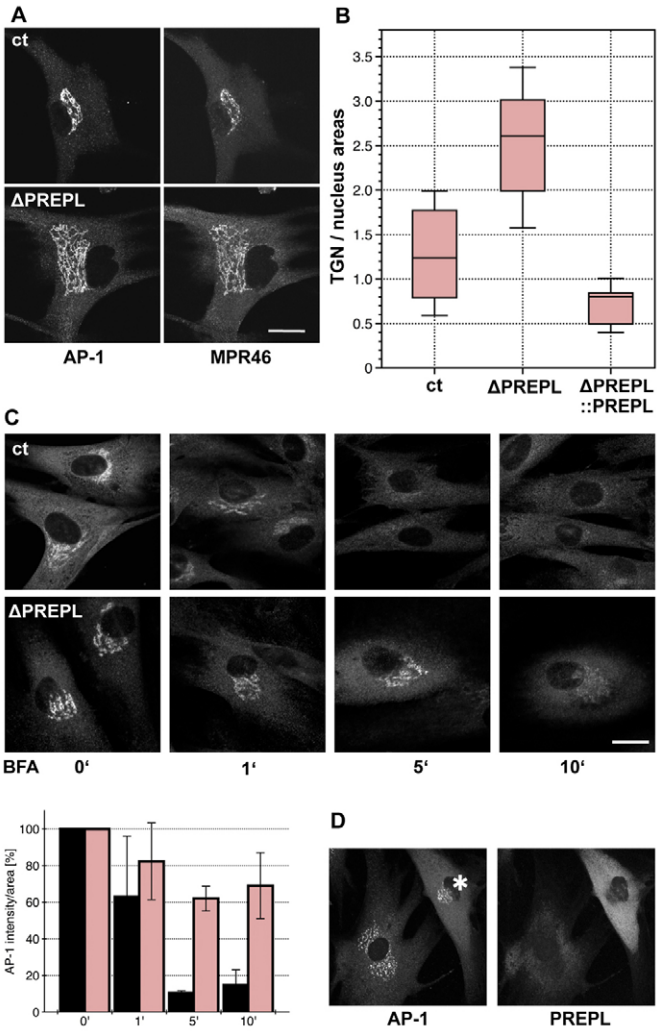

Fig. 7. AP-1 membrane binding in primary human fibroblasts of PREPL-deficient patients. (**A**) Colocalisation of AP-1 (anti-γ1) and the mannose-6-phosphate receptor MPR46 in the primary human control fibroblasts (ct 8) and PREPL-deficient primary human fibroblasts (HCS 16). (**B**) Quantification of the TGN size expressed as the TGN area relative to the nucleus area (ct $n=10$; ΔPREPL $n=9$; rescued $n=9$). (**C**) BFA (5 µg/ml)-induced redistribution of AP-1 (anti-γ1 staining) in human control fibroblasts (ct 8) and the PREPL-deficient human fibroblasts (HCS 16). BFA experiment with the two additional cell lines are shown in supplementary material Fig. S4B. Histogram shows quantification of the reduction in AP-1 membrane labelling (signal intensity normalised for the TGN area) in these four human cell lines. Black bars, wild type; pink, PREPL-deficient. (**D**) PREPL-HA expression in PREPL-deficient HCS 16 cells normalises TGN morphology (see quantification in B). Scale bars: 20 µm (A); 10 µm (C,D). Asterisk marks PREPL expression.

of 'accessory' proteins have been observed for several proteins in AP-2-mediated endocytosis, whereas only moderate decreases reveal phenotypes (Mettlen et al., 2009). The number of proteins involved in CCV formation and the complexity of their interaction network may readily allow adaptations increasing the robustness of the system. The expanded, spread out TGN could contribute to such an adaptation of the vesicle budding machinery as it increases the number of AP-1 docking and budding sites. The mannose-6-phosphate receptor MPR46 was found in all the TGN areas coated with AP-1 in the PREPL-deficient cells as in the controls (Fig. 7A). This, together with the intracellular pro-cathepsin D transport and the maintenance of the TGN morphology upon BFA treatment, indicates that the expansion does not lead to the formation of separated, functionally impaired TGN subdomains. However, the impaired GH secretion of the patients point to essential PREPL functions in regulated secretory pathways in the brain, in line with a function in AP-1-dependent pathways. This cell-type specific pathway will be analysed in detail in a PREPL mouse 'knockout' model. In summary, the absence of PREPL causes the same alterations of AP-1 membrane–cytoplasm recycling as replacing the N-terminal seventy amino acids of µ1A by those of µ2 (AP-1*).

Discussion

We identified the prolyl-oligopeptidase-like protein PREPL as a novel AP-1 complex effector. This is the first molecular function identified for PREPL. Low PREPL expression increase AP-1 membrane binding and increased PREPL expression reduces AP-1 membrane binding. PREPL's AP-1 effector function requires the N-terminal seventy amino acids of the µ1A-adaptin subunit. Exchanging this µ1A domain by the corresponding domain of the plasma membrane AP-2 complex µ2-adaptin, slows down recycling of this chimeric AP-1* complex and prevents PREPL-induced AP-1* redistribution. A large fraction of membrane bound AP-1* has no cargo proteins bound, indicating low-affinity membrane binding, but the redistribution of the complex into the cytoplasm is nevertheless reduced (Medigeshi et al., 2008). This is most likely mediated by the additional two major components mediating AP-1 membrane binding, Arf-1^{GTP} and PI-4-P. A pool of cargo-free, membrane bound AP-1 can be generated by stalled and aborted vesicle budding events. Formation of vesicles has to be regulated to ensure correct cargo sampling, precise budding kinetics and the correct formation of the 'zip-code' for the respective acceptor compartment. It involves a large number of proteins, which undergo multiple orchestrated interactions. Given the number of proteins involved and the complexity of the process, it is not surprising, that not all budding events are successful. This requires uncoating of partially assembled coats in order to recycle the proteins and to free the membrane enabling new rounds of transport vesicle formation (Liu et al., 2009; Loerke et al., 2011; Loerke et al., 2009; Schmid and McMahon, 2007; Taylor et al., 2011). Our data suggest that PREPL is involved in the uncoating of imperfect AP-1 coats. The cargo free AP complex open conformation seems to have a lower energy content than the closed one (Jackson et al., 2010). Therefore, PREPL binding to the wide γ1-µ1A-β1 cleft of the cargo-domain closed conformation could be required to overcome an energy barrier and to induce a less favoured AP-1 conformation with reduced affinity for membranes.

Two molecular mechanisms can be proposed based on the PREPL/AP-1 binding mode and the protein structures. Arf-1^{GTP} hydrolysis by Arf1-GAP requires the high membrane curvature induced by vesicle formation and thus Arf-1^{GTP} will not be inactivated, if vesicle formation is stalled (Ambroggio et al., 2010). Indeed, the AP-1 pool recycling independent of clathrin recycles slower than the AP-1 pool of CCV (Wu et al., 2003). Arf-1^{GTP} is bound by γ1 and β1 and the PI-4-P-binding site has been proposed to be part of γ1. The µ1A N-terminus is located at the bottom of a cleft formed by the two large γ1 and β1 adaptins (Fig. 1) and recruiting PREPL to this wide cleft of a cargo-free

Journal of Cell Science

AP-1 can induce conformational changes in both, which could weaken binding to Arf-1^{GTP} as well as to PI-4-P (Austin et al., 2000; Heldwein et al., 2004; Meyer et al., 2005; Wang et al., 2003). A second molecular mechanism would be the induction of conformational changes in the N-terminal domain of μ1A. The N-terminal seventy amino acids of μ1A are not in contact with the membrane, but the second half of the 150 aa long μ1A N-terminal globular domain faces the membrane and it facilitates the binding of μ1A to β1 (Heldwein et al., 2004). Conformational changes could be transferred onto this domain and onto β1 weakening Arf-1^{GTP} binding to β1 and also from β1 to γ1 weakening PI-4-P binding as well as Arf-1^{GTP} binding (Fig. 1; supplementary material Fig. S5). The molecular mechanism of PREPL in AP-1 recycling have to be analysed in structure–function experiments once the PREPL 3D structure has been resolved.

Interestingly, also the N-terminal domain of the polarised epithelia specific isoform of μ1A, the μ1B-adaptin, appears to have a function in regulating AP-1B complex membrane binding. An antibody directed against its N-terminal aa 44–56 inhibits AP-1B function. Moreover, it does not inhibit AP-1B in all cell lines, revealing even cell line and therefore most likely pathway specific mechanisms in regulating AP-1B functions (Cancino et al., 2007).

Although PREPL's AP-1 effector function can be demonstrated in fibroblasts, it appears only to be essential for specific AP-1 pathways. PREPL expression is highest in brain and it is expressed to a lesser extent in kidney, heart and skeletal muscle, whereas only trace amounts are found elsewhere. Disease syndromes of PREPL-deficient patients indicate that tissue specific AP-1 functions exist for which PREPL is indispensable (Jaeken et al., 2006). PREPL and SLC3A1 genes are mutated in patients with the hypotonia-cystinuria syndrome. It is associated with cystinuria type I, growth retardation, infantile hypotonia and anorexia and dysmorphy. Deficiency in SLC3A1 only causes cystinuria type I and thus the other phenotypes can be attributed to PREPL (Jaeken et al., 2006; Martens et al., 2006; Martens et al., 2008). This is also confirmed by a recently identified patient with point mutations only in the PREPL coding sequence (J. Creemers, unpublished results). This demonstrates essential PREPL functions in only this subset of tissues and indicates that the PREPL supported AP-1 membrane dissociation is crucial for specific AP-1 pathways in those tissues. These disease syndromes point to defects in regulated secretory pathways and AP-1 association with regulated secretory pathways has been demonstrated in other tissues (Lui-Roberts et al., 2005; Martin et al., 2000). It will be of special interest to investigate impaired secretion in GH producing somatotrophs or cells upstream in this pathway, like somatostatin or GH-releasing hormone-producing cells as HCS patients show hyposecretion of GH. A PREPL mouse 'knockout' model will allow to analyse these regulated secretory pathways.

Materials and Methods

Cell lines and cell culture

The μ1A-deficient mouse embryonic fibroblast cell line and the AP-1* expressing cell line have been described (Meyer et al., 2000). Human HCS fibroblasts have been described (Jaeken et al., 2006). Cell lines were cultured in DMEM (GIBCO, Karlsruhe, Germany) supplemented with 10% fetal calf serum (PAA, Cölbe, Germany). Hygromycin B (Calbiochem, Schwalbach, Germany) was added to the medium up to 500 mg/ml for the selection of stable transfectants. For routine culture hygromycin B was added to 200 mg/ml.

Antisera and microscopy

Cells were cooled, fixed with paraformaldehyde and permeabilised with saponin or fixed with cooled methanol following standard protocols. AP-1/AP-1*, AP-2 and clathrin were detected with anti-γ1, anti-α and anti-chc mouse monoclonal antibodies (BD Biosciences, Heidelberg, Germany). HA-tagged proteins were detected with a rat monoclonal antibody (Roche, Basel, Switzerland). Hsc70 was detected using a rat monoclonal antibody (1B5, Abcam, Cambridge, UK). Anti-MPR46 serum has been described (Meyer et al., 2000). Four murine PREPL peptides were injected into rabbits and only the peptide 235–250 aa was recognised by the serum. Specificity of the anti-PREPL serum is shown in Fig. 4 and supplementary material Fig. S4. Secondary antibodies were from Jackson ImmunoResearch. Confocal microscopy was performed using a Leica *DRM IRE2* TCS SP2 with a Plan Apochromat 63×/1.40 (Leica, Bensheim, Germany). Images were quantified using the Leica microscope and ImageJ software packages (NIH, USA). Diagrams were generated using DataGraph (Visual Data Tools, USA).

Y2H library screen

The yeast tester strain AH109 carrying auxotrophic markers *ADE2* und *HIS3* as Gal4p reporter genes was used in all experiments (Invitrogen, Darmstadt, Germany). The N-terminal seventy amino acid encoding μ1A and μ2 cDNA fragments were cloned into pGBT9 and the various prey constructs were cloned into pACT2 (Invitrogen, Darmstadt, Germany). 3-amino-1,2,4-triazole (3AT) competitive inhibitor for the His3 enzyme imidazoleglycerol-phosphate dehydratase. The mouse embryonic day 11.5 prey cDNA library has been described (Behrens et al., 1998). Growth of yeast strains on selective media was recorded at various time points after incubations at 30℃ over 5 days.

PREPL immunoprecipitation

Mouse brain extracts were prepared from cortex and brainstem separately in 100 mM MES pH 6.5, 1 mM EGTA, 0.5 mM $MgCl_2$, (vesicle buffer) protease inhibitor cocktail (Sigma, Selze, Germany) on ice. Cells were lysed by passing them subsequently through 20G and 24G needles, 10 times each. Extracts were cleared from cell debris by a 1000 ***g*** centrifugation, 4℃, 5 minutes and then spun at 10,000 or 14,000 ***g***, 10 minutes, 4℃. MEF cultures expressing either AP-1 or AP-1* were incubated with 0.1 mg/ml DSP (Dithiobis[succinimidyl propionate], Sigma, Selze, Germany) in PBS over 30 minutes at 4℃. After washing with Tris-buffer, cells were collected in vesicle buffer, lysed by sonication and 14,000 ***g*** pellet and supernatant fractions were prepared. 300 μl were incubated with 2 μl or without anti-PREPL antibody (mouse polyclonal, Abnova B01, Heidelberg, Germany) at 4℃ over 3 hours. Dynabeads Protein G (Dynal Biotech, Oslo, Norway) were washed with 100 mM NaOAc pH 5 according to the manufacturer's protocol. Extracts were adjusted to pH 5 with NaOAc and incubated with 15 μl Dynabeads suspension for 45 minutes at room temperature. Beads were washed three times with vesicle buffer and resuspended in SDS-PAGE loading buffer. Proteins were separated on 10% SDS-PAGE, blotted onto nitrocellulose membrane and PREPL was detected with the polyclonal rabbit anti-serum in PBS. Membranes were subsequently developed with anti-sera in PBS, 0,05% Tween 20 and the ECL luminescence detection kit (PICO; Pierce-ThermoScientific, Karlsruhe, Germany), recorded with a Fuji LAS 1000 (Fujifilm Corp., Düsseldorf, Germany) camera system.

PREPL 'knockdown'

PREPL 'knockdown' experiments were performed in HeLa cells. Four oligonucleotides of human PREPL were designed: MuL 1 5′-CCAAGUGUCUUCAGAAUAATTTTGGUUCACAGAAGUCUUAUU-3′; MuL 2 5′-CAAUGGCCUUGCUGAUUUATTTTGUUACCGGAACGACUAAAU-3′; MuL 3 5′-GUCGUUUCCUCACCAUAAATTTTCAGCAAAGGAGUGGUAUU-U-3′; MuL 4 5′-UCGAGGAUCUUAAGAAAUATTTTAGCUCCUAGAAUU-CUUUAU-3′ (IBA, Göttingen, Germany) (Reynolds et al., 2004). Cells were grown to sub-confluency in dishes of 10-cm diameter, transfected with Lipofectamin RNAi Max (Invitrogen, Darmstadt, Germany) and 600 pmol of the respective MuL or Lamin oligonucleotides.

Acknowledgements

We thank O. Bernhard and J. Wollenweber for technical assistance and W. Birchmeier (Berlin, Germany) for reagents.

Author contributions

K.R., J.B. and P.S. designed, performed and analysed experiments. J.C. isolated the patient cell lines. P.S. and J.C. wrote the manuscript.

Funding

This work is supported by the German Research Foundation (DFG) [grant numbers SFB 523/A6, 802/3-1 and 802/3-2 to P.S.]; and the

European Community's Seventh Framework Programme [grant number 223077 to J.C.]; and FWO Vlaanderen to J.C.

Supplementary material available online at
http://jcs.biologists.org/lookup/suppl/doi:10.1242/jcs.116079/-/DC1

References

Ambroggio, E., Sorre, B., Bassereau, P., Goud, B., Manneville, J. B. and Antonny, B. (2010). ArfGAP1 generates an Arf1 gradient on continuous lipid membranes displaying flat and curved regions. *EMBO J.* **29**, 292-303.

Austin, C., Hinners, I. and Tooze, S. A. (2000). Direct and GTP-dependent interaction of ADP-ribosylation factor 1 with clathrin adaptor protein AP-1 on immature secretory granules. *J. Biol. Chem.* **275**, 21862-21869.

Austin, C., Boehm, M. and Tooze, S. A. (2002). Site-specific cross-linking reveals a differential direct interaction of class 1, 2, and 3 ADP-ribosylation factors with adaptor protein complexes 1 and 3. *Biochemistry* **41**, 4669-4677.

Behrens, J., Jerchow, B. A., Würtele, M., Grimm, J., Asbrand, C., Wirtz, R., Kühl, M., Wedlich, D. and Birchmeier, W. (1998). Functional interaction of an axin homolog, conductin, with β-catenin, APC, and GSK3β. *Science* **280**, 596-599.

Cancino, J., Torrealba, C., Soza, A., Yuseff, M. I., Gravotta, D., Henklein, P., Rodriguez-Boulan, E. and González, A. (2007). Antibody to AP1B adaptor blocks biosynthetic and recycling routes of basolateral proteins at recycling endosomes. *Mol. Biol. Cell* **18**, 4872-4884.

Collins, B. M., McCoy, A. J., Kent, H. M., Evans, P. R. and Owen, D. J. (2002). Molecular architecture and functional model of the endocytic AP2 complex. *Cell* **109**, 523-535.

Conner, S. D. and Schmid, S. L. (2002). Identification of an adaptor-associated kinase, AAK1, as a regulator of clathrin-mediated endocytosis. *J. Cell Biol.* **156**, 921-929.

Dannhauser, P. N. and Ungewickell, E. J. (2012). Reconstitution of clathrin-coated bud and vesicle formation with minimal components. *Nat. Cell Biol.* **14**, 634-639.

Di Daniel, E., Glover, C. P., Grot, E., Chan, M. K., Sanderson, T. H., White, J. H., Ellis, C. L., Gallagher, K. T., Uney, J., Thomas, J. et al. (2009). Prolyl oligopeptidase binds to GAP-43 and functions without its peptidase activity. *Mol. Cell. Neurosci.* **41**, 373-382.

Doray, B. and Kornfeld, S. (2001). γ subunit of the AP-1 adaptor complex binds clathrin: implications for cooperative binding in coated vesicle assembly. *Mol. Biol. Cell* **12**, 1925-1935.

Gallusser, A. and Kirchhausen, T. (1993). The β 1 and β 2 subunits of the AP complexes are the clathrin coat assembly components. *EMBO J.* **12**, 5237-5244.

Ghosh, P. and Kornfeld, S. (2003). AP-1 binding to sorting signals and release from clathrin-coated vesicles is regulated by phosphorylation. *J. Cell Biol.* **160**, 699-708.

Glyvuk, N., Tsytsyura, Y., Geumann, C., D'Hooge, R., Hüve, J., Kratzke, M., Baltes, J., Böning, D., Klingauf, J. and Schu, P. (2010). AP-1/σ1B-adaptin mediates endosomal synaptic vesicle recycling, learning and memory. *EMBO J.* **29**, 1318-1330.

Heldwein, E. E., Macia, E., Wang, J., Yin, H. L., Kirchhausen, T. and Harrison, S. C. (2004). Crystal structure of the clathrin adaptor protein 1 core. *Proc. Natl. Acad. Sci. USA* **101**, 14108-14113.

Hirst, J., Sahlender, D. A., Li, S., Lubben, N. B., Borner, G. H. and Robinson, M. S. (2008). Auxilin depletion causes self-assembly of clathrin into membraneless cages in vivo. *Traffic* **9**, 1354-1371.

Höning, S., Ricotta, D., Krauss, M., Späte, K., Spolaore, B., Motley, A., Robinson, M., Robinson, C., Haucke, V. and Owen, D. J. (2005). Phosphatidylinositol-(4,5)-bisphosphate regulates sorting signal recognition by the clathrin-associated adaptor complex AP2. *Mol. Cell* **18**, 519-531.

Jackson, L. P., Kelly, B. T., McCoy, A. J., Gaffry, T., James, L. C., Collins, B. M., Höning, S., Evans, P. R. and Owen, D. J. (2010). A large-scale conformational change couples membrane recruitment to cargo binding in the AP2 clathrin adaptor complex. *Cell* **141**, 1220-1229.

Jaeken, J., Martens, K., Francois, I., Eyskens, F., Lecointre, C., Derua, R., Meulemans, S., Slootstra, J. W., Waelkens, E., de Zegher, F. et al. (2006). Deletion of PREPL, a gene encoding a putative serine oligopeptidase, in patients with hypotonia-cystinuria syndrome. *Am. J. Hum. Genet.* **78**, 38-51.

Liu, A. P., Loerke, D., Schmid, S. L. and Danuser, G. (2009). Global and local regulation of clathrin-coated pit dynamics detected on patterned substrates. *Biophys. J.* **97**, 1038-1047.

Lo, S. Y., Brett, C. L., Plemel, R. L., Vignali, M., Fields, S., Gonen, T. and Merz, A. J. (2011). Intrinsic tethering activity of endosomal Rab proteins. *Nat. Struct. Mol. Biol.* **19**, 40-47.

Loerke, D., Mettlen, M., Yarar, D., Jaqaman, K., Jaqaman, H., Danuser, G. and Schmid, S. L. (2009). Cargo and dynamin regulate clathrin-coated pit maturation. *PLoS Biol.* **7**, e57.

Loerke, D., Mettlen, M., Schmid, S. L. and Danuser, G. (2011). Measuring the hierarchy of molecular events during clathrin-mediated endocytosis. *Traffic* **12**, 815-825.

Lui-Roberts, W. W., Collinson, L. M., Hewlett, L. J., Michaux, G. and Cutler, D. F. (2005). An AP-1/clathrin coat plays a novel and essential role in forming the Weibel-Palade bodies of endothelial cells. *J. Cell Biol.* **170**, 627-636.

Martens, K., Derua, R., Meulemans, S., Waelkens, E., Jaeken, J., Matthijs, G. and Creemers, J. W. (2006). PREPL: a putative novel oligopeptidase propelled into the limelight. *Biol. Chem.* **387**, 879-883.

Martens, K., Jaeken, J., Matthijs, G. and Creemers, J. W. (2008). Multi-system disorder syndromes associated with cystinuria type I. *Curr. Mol. Med.* **8**, 544-550.

Martin, S., Ramm, G., Lyttle, C. T., Meerloo, T., Stoorvogel, W. and James, D. E. (2000). Biogenesis of insulin-responsive GLUT4 vesicles is independent of brefeldin A-sensitive trafficking. *Traffic* **1**, 652-660.

Medigeshi, G. R., Krikunova, M., Radhakrishnan, K., Wenzel, D., Klingauf, J. and Schu, P. (2008). AP-1 membrane-cytoplasm recycling regulated by μ1A-adaptin. *Traffic* **9**, 121-132.

Mettlen, M., Stoeber, M., Loerke, D., Antonescu, C. N., Danuser, G. and Schmid, S. L. (2009). Endocytic accessory proteins are functionally distinguished by their differential effects on the maturation of clathrin-coated pits. *Mol. Biol. Cell* **20**, 3251-3260.

Meyer, C., Zizioli, D., Lausmann, S., Eskelinen, E. L., Hamann, J., Saftig, P., von Figura, K. and Schu, P. (2000). μ1A-adaptin-deficient mice: lethality, loss of AP-1 binding and rerouting of mannose 6-phosphate receptors. *EMBO J.* **19**, 2193-2203.

Meyer, D. M., Crottet, P., Maco, B., Degtyar, E., Cassel, D. and Spiess, M. (2005). Oligomerization and dissociation of AP-1 adaptors are regulated by cargo signals and by ArfGAP1-induced GTP hydrolysis. *Mol. Biol. Cell* **16**, 4745-4754.

Motley, A. M., Berg, N., Taylor, M. J., Sahlender, D. A., Hirst, J., Owen, D. J. and Robinson, M. S. (2006). Functional analysis of AP-2 α and μ2 subunits. *Mol. Biol. Cell* **17**, 5298-5308.

Owen, D. J. and Evans, P. R. (1998). A structural explanation for the recognition of tyrosine-based endocytotic signals. *Science* **282**, 1327-1332.

Owen, D. J., Setiadi, H., Evans, P. R., McEver, R. P. and Green, S. A. (2001). A third specificity-determining site in μ 2 adaptin for sequences upstream of Yxx phi sorting motifs. *Traffic* **2**, 105-110.

Parvari, R., Gonen, Y., Alshafee, I., Buriakovsky, S., Regev, K. and Hershkovitz, E. (2005). The 2p21 deletion syndrome: characterization of the transcription content. *Genomics* **86**, 195-211.

Rapoport, I., Boll, W., Yu, A., Böcking, T. and Kirchhausen, T. (2008). A motif in the clathrin heavy chain required for the Hsc70/auxilin uncoating reaction. *Mol. Biol. Cell* **19**, 405-413.

Reynolds, A., Leake, D., Boese, Q., Scaringe, S., Marshall, W. S. and Khvorova, A. (2004). Rational siRNA design for RNA interference. *Nat. Biotechnol.* **22**, 326-330.

Ricotta, D., Conner, S. D., Schmid, S. L., von Figura, K. and Höning, S. (2002). Phosphorylation of the AP2 μ subunit by AAK1 mediates high affinity binding to membrane protein sorting signals. *J. Cell Biol.* **156**, 791-795.

Ricotta, D., Hansen, J., Preiss, C., Teichert, D. and Höning, S. (2008). Characterization of a protein phosphatase 2A holoenzyme that dephosphorylates the clathrin adaptors AP-1 and AP-2. *J. Biol. Chem.* **283**, 5510-5517.

Robinson, M. S. and Kreis, T. E. (1992). Recruitment of coat proteins onto Golgi membranes in intact and permeabilized cells: effects of brefeldin A and G protein activators. *Cell* **69**, 129-138.

Rohde, G., Wenzel, D. and Haucke, V. (2002). A phosphatidylinositol (4,5)-bisphosphate binding site within mu2-adaptin regulates clathrin-mediated endocytosis. *J. Cell Biol.* **158**, 209-214.

Schmid, E. M. and McMahon, H. T. (2007). Integrating molecular and network biology to decode endocytosis. *Nature* **448**, 883-888.

Shan, L., Mathews, I. I. and Khosla, C. (2005). Structural and mechanistic analysis of two prolyl endopeptidases: role of interdomain dynamics in catalysis and specificity. *Proc. Natl. Acad. Sci. USA* **102**, 3599-3604.

Shinotsuka, C., Yoshida, Y., Kawamoto, K., Takatsu, H. and Nakayama, K. (2002). Overexpression of an ADP-ribosylation factor-guanine nucleotide exchange factor, BIG2, uncouples brefeldin A-induced adaptor protein-1 coat dissociation and membrane tubulation. *J. Biol. Chem.* **277**, 9468-9473.

Szeltner, Z., Rea, D., Renner, V., Fulop, V. and Polgar, L. (2002). Electrostatic effects and binding determinants in the catalysis of prolyl oligopeptidase. Site specific mutagenesis at the oxyanion binding site. *J. Biol. Chem.* **277**, 42613-42622.

Szeltner, Z., Alshafee, I., Juhász, T., Parvari, R. and Polgár, L. (2005). The PREPL A protein, a new member of the prolyl oligopeptidase family, lacking catalytic activity. *Cell. Mol. Life Sci.* **62**, 2376-2381.

Taylor, M. J., Perrais, D. and Merrifield, C. J. (2011). A high precision survey of the molecular dynamics of mammalian clathrin-mediated endocytosis. *PLoS Biol.* **9**, e1000604.

Ungewickell, E. J. and Hinrichsen, L. (2007). Endocytosis: clathrin-mediated membrane budding. *Curr. Opin. Cell Biol.* **19**, 417-425.

Wang, Y. J., Wang, J., Sun, H. Q., Martinez, M., Sun, Y. X., Macia, E., Kirchhausen, T., Albanesi, J. P., Roth, M. G. and Yin, H. L. (2003). Phosphatidylinositol 4 phosphate regulates targeting of clathrin adaptor AP-1 complexes to the Golgi. *Cell* **114**, 299-310.

Wu, X., Zhao, X., Puertollano, R., Bonifacino, J. S., Eisenberg, E. and Greene, L. E. (2003). Adaptor and clathrin exchange at the plasma membrane and trans-Golgi network. *Mol. Biol. Cell* **14**, 516-528.